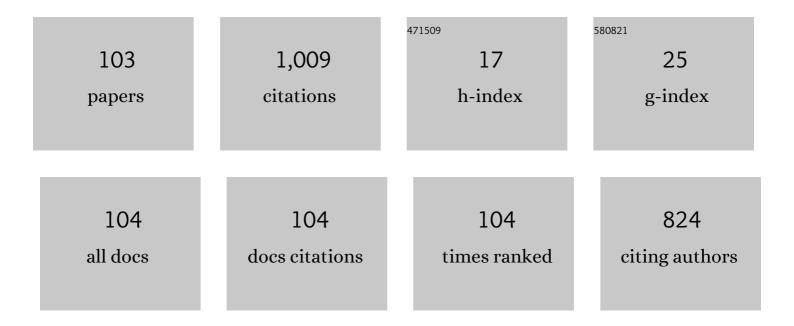
Hong-Xing Wang

List of Publications by Year in descending order

Source: https://exaly.com/author-pdf/3776000/publications.pdf Version: 2024-02-01



#	Article	IF	CITATIONS
1	Fabrication of UV Photodetector on TiO2/Diamond Film. Scientific Reports, 2015, 5, 14420.	3.3	81
2	An Enhancement-Mode Hydrogen-Terminated Diamond Field-Effect Transistor With Lanthanum Hexaboride Gate Material. IEEE Electron Device Letters, 2020, 41, 585-588.	3.9	52
3	UV-photodetector based on NiO/diamond film. Applied Physics Letters, 2018, 112, .	3.3	42
4	Normally-off hydrogen-terminated diamond field-effect transistor with Al2O3 dielectric layer formed by thermal oxidation of Al. Diamond and Related Materials, 2018, 81, 113-117.	3.9	39
5	Normally Off Hydrogen-Terminated Diamond Field-Effect Transistor With Ti/TiO _x Gate Materials. IEEE Transactions on Electron Devices, 2020, 67, 4784-4788.	3.0	28
6	Normally-off hydrogen-terminated diamond field effect transistor with yttrium gate. Carbon, 2021, 176, 307-312.	10.3	28
7	Fabrication of three dimensional diamond ultraviolet photodetector through down-top method. Applied Physics Letters, 2016, 109, 153507.	3.3	27
8	Photovoltaic Three-Dimensional Diamond UV Photodetector With Low Dark Current and Fast Response Speed Fabricated by Bottom-Up Method. IEEE Electron Device Letters, 2019, 40, 1186-1189.	3.9	27
9	Controllable hybrid shape of correlation and squeezing. Physical Review A, 2016, 94, .	2.5	24
10	Fabrication of monolithic diamond photodetector with microlenses. Optics Express, 2017, 25, 31586.	3.4	23
11	LiF/Alâ,,Oâ,ƒ as Dielectrics for MOSFET on Single Crystal Hydrogen-Terminated Diamond. IEEE Electron Device Letters, 2020, 41, 808-811.	3.9	21
12	Efficient and Tunable Photoinduced Honeycomb Lattice in an Atomic Ensemble. Laser and Photonics Reviews, 2018, 12, 1800050.	8.7	20
13	Iridium size effects in localized surface plasmon-enhanced diamond UV photodetectors. Applied Surface Science, 2019, 487, 674-677.	6.1	19
14	Enhanced ultraviolet photoresponse of diamond photodetector using patterned diamond film and two-step growth process. Materials Science in Semiconductor Processing, 2019, 89, 110-115.	4.0	19
15	Enhanced Responsivity of Diamond UV Detector Based on Regrown Lens Structure. IEEE Electron Device Letters, 2020, 41, 1829-1832.	3.9	19
16	Soil Evaporation and its Affecting Factors under Crop Canopy. Communications in Soil Science and Plant Analysis, 2007, 38, 259-271.	1.4	18
17	Diamond MIP structure Schottky diode with different drift layer thickness. Diamond and Related Materials, 2017, 73, 15-18.	3.9	18
18	Two-dimensional Talbot self-imaging via Electromagnetically induced lattice. Scientific Reports, 2017, 7, 41790.	3.3	17

#	Article	IF	CITATIONS
19	Enhanced ultraviolet absorption in diamond surface via localized surface plasmon resonance in palladium nanoparticles. Applied Surface Science, 2019, 464, 455-457.	6.1	17
20	Photoelectrical characteristics of ultra thin TiO 2 /diamond photodetector. Materials Letters, 2017, 188, 52-54.	2.6	16
21	Responsivity improvement of Ti–diamond–Ti structured UV photodetector through photocurrent gain. Optics Express, 2018, 26, 17092.	3.4	16
22	Diamond Schottky barrier diodes with floating metal rings for high breakdown voltage. Materials Science in Semiconductor Processing, 2019, 97, 101-105.	4.0	16
23	Hydrogen-terminated diamond field-effect transistor with AlOx dielectric layer formed by autoxidation. Scientific Reports, 2019, 9, 5192.	3.3	16
24	Fabrication of dual-termination Schottky barrier diode by using oxygen-/fluorine-terminated diamond. Applied Surface Science, 2018, 457, 411-416.	6.1	14
25	Performance of hydrogen-terminated diamond MOSFET with bilayer dielectrics of YSZ/Al2O3. Diamond and Related Materials, 2019, 99, 107532.	3.9	13
26	Room temperature direct bonding of diamond and InGaP in atmospheric air. Functional Diamond, 2021, 1, 110-116.	3.8	13
27	xmlns:mml="http://www.w3.org/1998/Math/MathML" id="M1"> <mml:mrow><mml:msub><mml:mrow><mml:mi mathvariant="normal">S</mml:mi><mml:mi mathvariant="normal">i<mml:mi mathvariant="normal">N</mml:mi </mml:mi </mml:mrow><mml:mrow><mml:mi>x</mml:mi></mml:mrow><td>2.7</td><td>12</td></mml:msub></mml:mrow>	2.7	12
28	Layers. Journal of Nanomaterials, 2015, 2015, 1-5. Ohmic contact between iridium film and hydrogen-terminated single crystal diamond. Scientific Reports, 2017, 7, 12157.	3.3	12
29	Room temperature bonding of Si and Si wafers by using Mo/Au nano-adhesion layers. Microelectronic Engineering, 2019, 215, 111018.	2.4	12
30	Adjustable charge states of nitrogen-vacancy centers in low-nitrogen diamond after electron irradiation and subsequent annealing. Applied Physics Letters, 2020, 117, .	3.3	12
31	Effect of depth of Buried-In Tungsten Electrodes on Single Crystal Diamond Photodetector. MRS Advances, 2016, 1, 1099-1104.	0.9	11
32	Annealing and lateral migration of defects in IIa diamond created by near-threshold electron irradiation. Applied Physics Letters, 2017, 110, .	3.3	11
33	Analysis of diamond pseudo-vertical Schottky barrier diode through patterning tungsten growth method. Applied Physics Letters, 2018, 112, .	3.3	11
34	Triple-mode squeezing with dressed six-wave mixing. Scientific Reports, 2016, 6, 25554.	3.3	10
35	Fabrication and Characterization of (100)â€Oriented Singleâ€Crystal Diamond p–i–n Junction Ultraviolet Detector. Physica Status Solidi (A) Applications and Materials Science, 2020, 217, 2000207.	1.8	9
36	Electrical properties of yttrium gate hydrogen-terminated diamond field effect transistor with Al2O3 dielectric layer. Applied Physics Letters, 2021, 118, .	3.3	9

#	Article	IF	CITATIONS
37	Characterization of UV photodetector based on ZnO/diamond film. Optics Express, 2019, 27, 36750.	3.4	9
38	FEM thermal analysis of Cu/diamond/Cu and diamond/SiC heat spreaders. AIP Advances, 2017, 7, 035102.	1.3	8
39	Performance Improved Vertical Diamond Schottky Barrier Diode With Fluorination-Termination Structure. IEEE Electron Device Letters, 2019, 40, 1229-1232.	3.9	8
40	Fabrication of Diamond Submicron Lenses and Cylinders by ICP Etching Technique with SiO2 Balls Mask. Materials, 2019, 12, 1622.	2.9	8
41	Fabrication of micro lens array on diamond surface. AIP Advances, 2019, 9, .	1.3	8
42	Temperature dependence of optical centres in ultrapure diamond after 200 keV electron irradiation. Journal Physics D: Applied Physics, 2020, 53, 135303.	2.8	8
43	Effects of surface activation time on Si-Si direct wafer bonding at room temperature. Materials Research Express, 2021, 8, 085901.	1.6	8
44	Performance-Improved Vertical Zr/Diamond Schottky Barrier Diode With Lanthanum Hexaboride Interfacial Layer. IEEE Electron Device Letters, 2021, 42, 1366-1369.	3.9	8
45	Self-powered diamond ultraviolet photodetector with a transparent Ag nanowire electrode. Nanotechnology, 2019, 30, 325204.	2.6	7
46	Enhancing diamond NV center density in HPHT substrate and epitaxy lateral overgrowth layer by tungsten pattern. Materials Letters, 2019, 240, 233-237.	2.6	7
47	Local initial heteroepitaxial growth of diamond (111) on Ru (0001)/c-sapphire by antenna-edge-type microwave plasma chemical vapor deposition. Applied Physics Letters, 2020, 117, .	3.3	7
48	Pd nanoparticle size effects in localized surface plasmon-enhanced diamond photodetectors. Optical Materials, 2020, 107, 110031.	3.6	7
49	Heteroepitaxy of single crystal diamond on Ir buffered KTaO3 (001) substrates. Applied Physics Letters, 2021, 119, .	3.3	7
50	Schottky Barrier Height Modulation of Zr/p-Diamond Schottky Contact by Inserting Ultrathin Atomic Layer-Deposited Al ₂ O ₃ . IEEE Transactions on Electron Devices, 2021, 68, 5995-6000.	3.0	7
51	FEM thermal and stress analysis of bonded GaN-on-diamond substrate. AIP Advances, 2017, 7, 095105.	1.3	6
52	Development of an all-optical framing camera and its application on the Z-pinch. Optics Express, 2017, 25, 32074.	3.4	6
53	Ohmic Contact of Pt/Au on Hydrogen-Terminated Single Crystal Diamond. Coatings, 2019, 9, 539.	2.6	6
54	Reducing Threading Dislocations of Single-Crystal Diamond via In Situ Tungsten Incorporation. Materials, 2022, 15, 444.	2.9	6

#	Article	IF	CITATIONS
55	Solution-processed tin oxide thin film for normally-off hydrogen terminated diamond field effect transistor. Applied Physics Letters, 2022, 120, .	3.3	6
56	Argon Ion Beam Current Dependence of Si-Si Surface Activated Bonding. Materials, 2022, 15, 3115.	2.9	6
57	Investigation of an InP-based image converter with optical excitation. Review of Scientific Instruments, 2017, 88, 033109.	1.3	5
58	FEM thermal analysis of high power GaN-on-diamond HEMTs. Journal of Semiconductors, 2018, 39, 104005.	3.7	5
59	RF Performance of Hydrogenated Single Crystal Diamond MOSFETs. , 2019, , .		5
60	3D TiO 2 /Diamond Ultraviolet Detector Using Backâ€ŧoâ€Back Pd Schottky Electrode. Physica Status Solidi (A) Applications and Materials Science, 2020, 217, 2000218.	1.8	5
61	Surface Morphology and Microstructure Evolution of Single Crystal Diamond during Different Homoepitaxial Growth Stages. Materials, 2021, 14, 5964.	2.9	5
62	Large <i>V</i> _{TH} of Normally-OFF Field Effect Transistor With Yttrium Gate Material Directly Deposited on Hydrogen-Terminated Diamond. IEEE Transactions on Electron Devices, 2022, 69, 3563-3567.	3.0	5
63	Small Subthreshold Swing Diamond Field Effect Transistors With SnO ₂ Gate Dielectric. IEEE Transactions on Electron Devices, 2022, 69, 4427-4431.	3.0	5
64	Effect of thermoelastic damping on silicon, GaAs, diamond and SiC micromechanical resonators. AIP Advances, 2017, 7, .	1.3	4
65	Investigating non-equilibrium carrier lifetimes in nitrogen-doped and boron-doped single crystal HPHT diamonds with an optical method. Applied Physics Letters, 2018, 112, 022103.	3.3	4
66	Schottky barrier diode fabricated on oxygen-terminated diamond using a selective growth approach. Diamond and Related Materials, 2019, 99, 107529.	3.9	4
67	Hydrogen-terminated diamond field-effect transistor with a bilayer dielectric of HfSiO4/Al2O3. Diamond and Related Materials, 2019, 99, 107530.	3.9	4
68	Diamond field effect transistors using bilayer dielectrics Yb2TiO5/Al2O3 on hydrogen-terminated diamond. Diamond and Related Materials, 2020, 106, 107866.	3.9	4
69	Hydrogen-terminated diamond field-effect transistor with a bilayer dielectric of HfSiON/Al2O3. AIP Advances, 2020, 10, 035327.	1.3	4
70	Fabrication of Dual-Barrier Planar Structure Diamond Schottky Diodes by Rapid Thermal Annealing. IEEE Transactions on Electron Devices, 2021, 68, 1176-1180.	3.0	4
71	Fabrication of a Micron-Scale Three-Dimensional Single Crystal Diamond Channel Using a Micro-Jet Water-Assisted Laser. Materials, 2021, 14, 3006.	2.9	4
72	A finite element analysis of the effects of geometrical shape on the elastic properties of chemical vapor deposited diamond nanowire. AIP Advances, 2017, 7, .	1.3	3

#	Article	IF	CITATIONS
73	Nonlinear optical induced lattice in atomic configurations. Scientific Reports, 2020, 10, 13396.	3.3	3
74	Visible-Light Activation of Photocatalytic for Reduction of Nitrogen to Ammonia by Introducing Impurity Defect Levels into Nanocrystalline Diamond. Materials, 2020, 13, 4559.	2.9	3
75	Hydrophobic Surface Coating of Nanodiamonds by Polyglycerolâ€Based Polymers with Alkyl Chains for Dispersing in an Organic Solvent. ChemNanoMat, 2020, 6, 1332-1336.	2.8	3
76	Nanocone Structures Enhancing Nitrogen-Vacancy Center Emissions in Diamonds. Coatings, 2020, 10, 513.	2.6	3
77	Temperature dependent thermal conductivity of IIa diamond by laser excited Raman spectroscopy. Applied Physics Letters, 2021, 118, 192104.	3.3	3
78	Simple way to fabricate orderly arranged nanostructure arrays on diamond utilizing metal dewetting effect. Optics Express, 2021, 29, 28359.	3.4	3
79	Performance of hydrogen-terminated diamond MOSFET with LaB6/Al2O3 bilayer dielectric. Diamond and Related Materials, 2021, 120, 108646.	3.9	3
80	Electrical and Thermal Characteristics of AlGaN/GaN HEMT Devices with Dual Metal Gate Structure: A Theoretical Investigation. Materials, 2022, 15, 3818.	2.9	3
81	Creation and Migration of Intrinsic Defects in Siâ€Doped Diamond Produced Using Microwave Plasma Chemical Vapor Deposition. Physica Status Solidi (A) Applications and Materials Science, 2019, 216, 1900003.	1.8	2
82	Diamond avalanche diodes for obtaining high-voltage pulse with subnanosecond front edge. AIP Advances, 2020, 10, .	1.3	2
83	Suppressing Nitrogen-Vacancy Centers to Enhance Performance of Diamond Ultraviolet Photodetector via Growing With Tungsten. IEEE Transactions on Electron Devices, 2021, 68, 6228-6232.	3.0	2
84	Influence of near threshold energy electron irradiation on the thermal conductivity of IIa diamond. Applied Physics Letters, 2021, 119, 182105.	3.3	2
85	Structural changes during femtosecond laser percussion drilling of high-aspect-ratio diamond microholes. Optical Engineering, 2022, 61, .	1.0	2
86	Normally-off hydrogen-terminated diamond field effect transistor with a bilayer dielectric of Er2O3/Al2O3. Diamond and Related Materials, 2022, 123, 108848.	3.9	2
87	A 3 W High-Voltage Single-Chip Green Light-Emitting Diode with Multiple-Cells Network. Journal of Nanomaterials, 2015, 2015, 1-4.	2.7	1
88	Hybrid Three-Mode Correlation and Squeezing in a Pr3+:YSO Crystal. Scientific Reports, 2017, 7, 1743.	3.3	1
89	Thickness Impact on the Morphology, Strain Relaxation and Defects of Diamond Heteroepitaxially Grown on Ir/Al2O3 Substrates. Materials, 2022, 15, 624.	2.9	1
90	The influence of nitrogen doping on the thermal conductivity of diamond heat sink. Spectroscopy Letters, 0, , 1-6.	1.0	1

#	Article	IF	CITATIONS
91	Electrical Characteristics of Diamond MOSFET with 2DHG on a Heteroepitaxial Diamond Substrate. Materials, 2022, 15, 2557.	2.9	1
92	Transport Properties of the Two-Dimensional Hole Gas for H-Terminated Diamond with an Al2O3 Passivation Layer. Crystals, 2022, 12, 390.	2.2	1
93	Detection of Glucose Using Diamond Solution-Gate Field-Effect Transistor. IEEE Transactions on Electron Devices, 2022, 69, 4534-4539.	3.0	1
94	Leakage current reduction of normally off hydrogen-terminated diamond field effect transistor utilizing dual-barrier Schottky gate. Journal of Applied Physics, 2022, 132, .	2.5	1
95	Optical defects and their depth penetration in 200 keV electron irradiated IIa diamond. Radiation Effects and Defects in Solids, 2020, 175, 1083-1092.	1.2	0
96	The role of tunable nonlinear dark resonances on vacuum Rabi splitting and optical bistability in an atom-cavity system. Scientific Reports, 2021, 11, 10503.	3.3	0
97	Operation of Diamond Solution-Gated Field-Effect Transistor in the Frequency Domain. IEEE Transactions on Electron Devices, 2021, , 1-7.	3.0	0
98	A Method for Demonstration of the Feasibility of InP as an All-optical Imaging Sensor. , 2018, , .		0
99	Progress of diamond substrate development. , 2021, , .		0
100	Room Temperature Bonding of Semiconductor Materials Based on Mo/Au Interlayer. , 2021, , .		0
101	Effect of HfO2-Based Multi-Dielectrics on Electrical Properties of Amorphous In-Ga-Zn-O Thin Film Transistors. Coatings, 2021, 11, 1381.	2.6	0
102	HfAlOx/Al2O3 Bilayer Dielectrics for a Field Effect Transistor on a Hydrogen-Terminated Diamond. Materials, 2022, 15, 446.	2.9	0
103	Tunable Continuousâ€Variable Tripartite Entanglement via Cascaded Thirdâ€Order Nonlinear Processes in a Ring Cavity. Annalen Der Physik, 2022, 534, 2100396.	2.4	0